Human Pathology (2019) **83**, 59–67

ELSEVIER

Human PATHOLOGY

www.elsevier.com/locate/humpath

Original contribution

SMARCB1 (INI1)–deficient sinonasal carcinoma: a series of 13 cases with assessment of histologic patterns☆

Aanchal Kakkar MD[a], Vijay Mariadas Antony MBBS[a], Raja Pramanik MD, DM[b], Pirabu Sakthivel MS[c], Chirom Amit Singh MS[c], Deepali Jain MD, FIAC[a,*]

[a]*Department of Pathology, All India Institute of Medical Sciences, New Delhi 110029, India*
[b]*Department of Medical Oncology, All India Institute of Medical Sciences, New Delhi 110029, India*
[c]*Department of Otorhinolaryngology and Head and Neck Surgery, All India Institute of Medical Sciences, New Delhi 110029, India*

Received 20 April 2018; revised 3 August 2018; accepted 9 August 2018

Keywords:
Sinonasal carcinoma;
SMARCB1/ INI1;
Basaloid;
Rhabdoid;
Plasmacytoid;
Oncocytic

Summary A significant proportion of sinonasal malignancies comprise poorly differentiated/undifferentiated carcinomas that defy accurate histologic classification and behave aggressively. Recent years have seen a refinement of this spectrum by inclusion of novel entities harboring specific genetic alterations, including SMARCB1 (INI1)–deficient sinonasal carcinoma (SDSC), characterized by inactivating alterations in *SMARCB1* gene, as demonstrated by loss of INI1 immunoexpression. Cyclin D1 is a cell-cycle regulatory protein downstream of INI1. Loss of INI1 leads to derepression of cyclin D1 transcription, suggesting its role as a putative therapeutic target. However, cyclin D1 expression has not been assessed in SDSCs. We retrieved all sinonasal carcinomas, including sinonasal undifferentiated carcinoma, undifferentiated carcinoma, poorly differentiated squamous cell carcinoma, and adenocarcinoma. Histopathologic features were reviewed. INI1 immunohistochemistry was performed. Cyclin D1 was performed in cases showing INI1 loss. Loss of INI1 staining was seen in 13 cases (5.8%), including 11 males and 2 females (age range, 11-65 years). Original diagnoses included SDSC (3/13), sinonasal undifferentiated carcinoma (3/13), adenocarcinoma (3/13), poorly differentiated squamous cell carcinoma (2/13), and poorly differentiated carcinoma (2/13). Tumors were predominantly basaloid in 6 cases and plasmacytoid/rhabdoid in 5 cases. We identified 2 cases having oncocytoid cells arranged in a gland-like pattern. Significant cyclin D1 immunoexpression was absent. SDSC is a rare, emerging entity that resembles a poorly differentiated carcinoma. Histomorphologic spectrum of these tumors is evolving. In addition to basaloid and plasmacytoid/rhabdoid cells, oncocytoid/adenocarcinoma-like pattern can also be seen in SDSC and predicts INI1 loss. These histologic patterns can further be subjected to INI1 immunohistochemistry for correct diagnosis.

1. Introduction

The sinonasal tract plays host to a wide variety of epithelial neoplasms. Although a proportion of them are the easily identifiable squamous cell carcinomas (SCCs), a major chunk of these are poorly differentiated or undifferentiated carcinomas that

☆ Disclosures: The authors have no competing interest to disclose. This research did not receive any specific grant from funding agencies in the public, commercial, or not-for-profit sectors

* Corresponding author at: Department of Pathology, All India Institute of Medical Sciences, New Delhi 110029, India.
E-mail address: deepalijain76@gmail.com (D. Jain).

https://doi.org/10.1016/j.humpath.2018.08.008
0046-8177/

defy accurate histologic classification and have variably aggressive biological behavior. In recent years, the spectrum of these neoplasms has been refined to a certain extent by the inclusion of newly described entities that harbor specific genetic alterations, for example, nuclear protein in testis (NUT) midline carcinoma, or are caused by oncogenic viruses, for example, human papillomavirus–related multiphenotypic carcinoma [1-4]. One such recently described entity is *SMARCB1* (INI1)–

Table 1 Clinicoradiological data, initial histopathology diagnosis, and clinical course of patients with *SMARCB1*-deficient sinonasal carcinoma

Case no.	Age (y)/ sex	Presenting complaints	Clinical and imaging findings	Initial diagnosis	Clinical course
1	23/ M	Nasal stuffiness × 5 mo; epistaxis × 4 mo; upper jaw pain, loosening of teeth × 4 mo; diminished vision × 3 mo	Soft tissue mass filling the left nasal cavity, maxillary and ethmoid sinuses with destruction of bony walls and floor of maxillary sinus	SNUC	Biopsy followed by 2 NACT (cisplatin + 5FU) with significant reduction in size of mass; followed by radical maxillectomy and PORT 60 Gy in 30 fractions; achieved CR; NED at 17 mo
2	60/ M	N/A	Mass in the left nasal cavity	SNUC	Biopsy only; no follow-up information available
3	40/ M	N/A	Polypoidal mass in the left nasal cavity	Sinonasal non–intestinal-type adenocarcinoma	Biopsy only; no follow-up information available
4	11/ M	Bilateral proptosis × 2 mo; decreased vision in both eyes × 1.5 mo; progressive facial distortion × 2 mo, epistaxis × 1 mo	8.5-cm bilateral nasal cavity mass extending into the ethmoid, maxillary sinuses, orbit, with destruction of lateral nasal walls, upper alveolus, clivus; infiltration into the skull base, cavernous sinus, basifrontal and temporal lobes	PDCA	Biopsy followed by NACT (cisplatin + 5FU) with subjective reduction in size of mass; to be followed by surgery and PORT at referring local hospital
5	58/ M	Pain and epistaxis × 1 mo	Polypoidal mass in the left nasal cavity	SMARCB1-deficient carcinoma	Biopsy from left nasal cavity mass followed by left lateral rhinotomy excision, 7 cycles of cisplatin, and PORT 60 Gy in 30 fractions; NED at 8 mo
6	65/F	Proptosis, vision loss × 1 mo	Friable growth in the nasal cavity	PDSCC	Biopsy only; no follow-up information available
7	31/ M	Nasal obstruction × 1 mo; vision loss × 15 d	Mass in the right middle turbinate, middle meatus, orbit	PDCA	Biopsy only; no follow-up information available
8	40/ M	N/A	Vascular mass in the right nasal cavity	SNUC	Biopsy only; no follow-up information available
9	47/F	Left nasal obstruction and discharge × 4 mo	Mass in the left nasal cavity	PDSCC	Biopsy only; no follow-up information available
10	64/ M	Left eye pain × 15 d, diplopia	Fleshy mass filling the nasal cavity, with intracranial extension on CT	Adenocarcinoma	Biopsy only; no follow-up information available
11	50/ M	Left-sided nasal obstruction, epistaxis × 5–6 mo	Left nasal cavity mass	Poorly differentiated adenocarcinoma	Biopsy only; no follow-up information available
12	20/ M	Right cheek swelling × 2 y; underwent surgery elsewhere 1 y ago; recurrent intractable nasal bleeding × 3 mo	Nasal cavity, right maxillary mass extending to the infratemporal fossa, skull base, orbit	SMARCB1-deficient carcinoma	Biopsy from maxillary antrum and medial wall; planned for palliative chemotherapy, but died of excessive bleeding and tumor progression 2 mo after diagnosis
13	37/ M	Right nasal obstruction, right eye proptosis and decreased vision × 1 mo	Right nasal cavity, right orbit, anterior skull base mass with intracranial extension to the frontal lobe	SMARCB1-deficient carcinoma	Biopsy only; planned for NACT followed by craniofacial resection and postoperative chemoradiation

Abbreviations: CR, clinical remission; 5FU, 5-fluorouracil; N/A, not available; NED, no evidence of disease; PDCA, poorly differentiated carcinoma; PDSCC, poorly differentiated SCC.

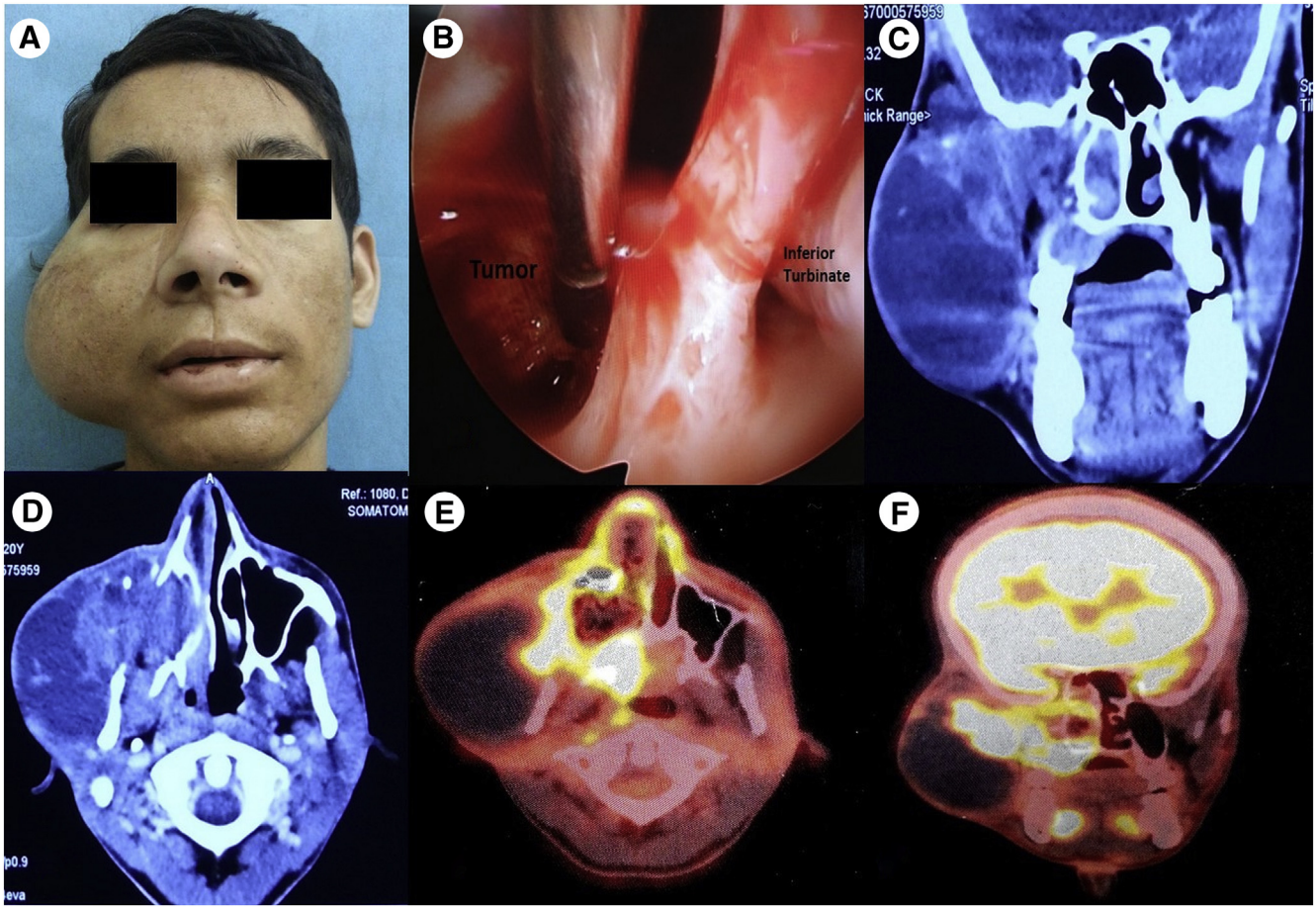

Fig. 1 Clinical and radiologic features for patient 12. A, External appearance at presentation. B, Endoscopic view of the tumor within the maxillary sinus. Coronal (C) and axial (D) contrast-enhanced CT images showing a heterogeneously enhancing lesion arising from right lateral wall of the nose, extending into the nasal cavity, maxilla, masticator, and buccal space (infratemporal fossa), and abutting the masticator muscles and parotid gland. Superiorly, the lesion is extending into the extraconal compartment of orbit and abutting the inferior rectus muscle. Large cystic areas are seen in the masticator and buccal space (infratemporal fossa) with enhancement. Axial (E) and coronal (F) positron-emission tomographic/CT images show a metabolically active soft tissue density mass arising from the right maxilla with similar extensions, few enlarged right level 1b lymph nodes and right submandibular gland with increased [^{18}F]-fluorodeoxyglucose activity, suggestive of disease involvement.

deficient sinonasal carcinoma (SDSC), which is characterized by inactivating alterations in *SMARCB1*, a tumor suppressor gene located on 22q11.2, as demonstrated by loss of INI1 immunoexpression, as well as morphologic evidence of rhabdoid differentiation [5,6]. Less than 60 cases of this novel entity have been described in the literature, with the largest series being of 39 cases and including only 1 case reported from Asia and none from the Indian subcontinent [5-8].

The initial description of SDSC by Agaimy et al [5] was that of basaloid-appearing tumors closely resembling basaloid SCC, with interspersed isolated rhabdoid appearing cells. Bishop et al [6], apart from this typical morphologic pattern, described cases in which rhabdoid cells or plasmacytoid-appearing cells made up the bulk of the tumor. They also reported the identification of pseudoglandular spaces, but tubules/glandular structures were not recognized in either of these initial reports. Subsequently, glandular architecture was reported in more recently identified cases [7,9]. Thus, as more cases are encountered, newer morphologic patterns are being revealed.

Loss of INI1 in rhabdoid tumors of the nervous system, that is, atypical teratoid/rhabdoid tumor (AT/RT) has been associated with derepression of cyclin D1 transcription [10,11]. Cyclin D1 is a cell-cycle regulatory protein, and its overexpression leads to progression of the cell cycle, with subsequent cell proliferation [10,11]. Thus, cyclin D1 is considered a putative therapeutic target in RTs [12]. Although cyclin D1 immunoexpression has been assessed in AT/RTs [13], its expression in SDSCs has not been evaluated. Therefore, we describe a series of cases of SDSC diagnosed retrospectively by INI1 immunohistochemistry (IHC), which is the first reported series of this enigmatic tumor from India, and report results of immunostaining for cyclin D1 in this tumor.

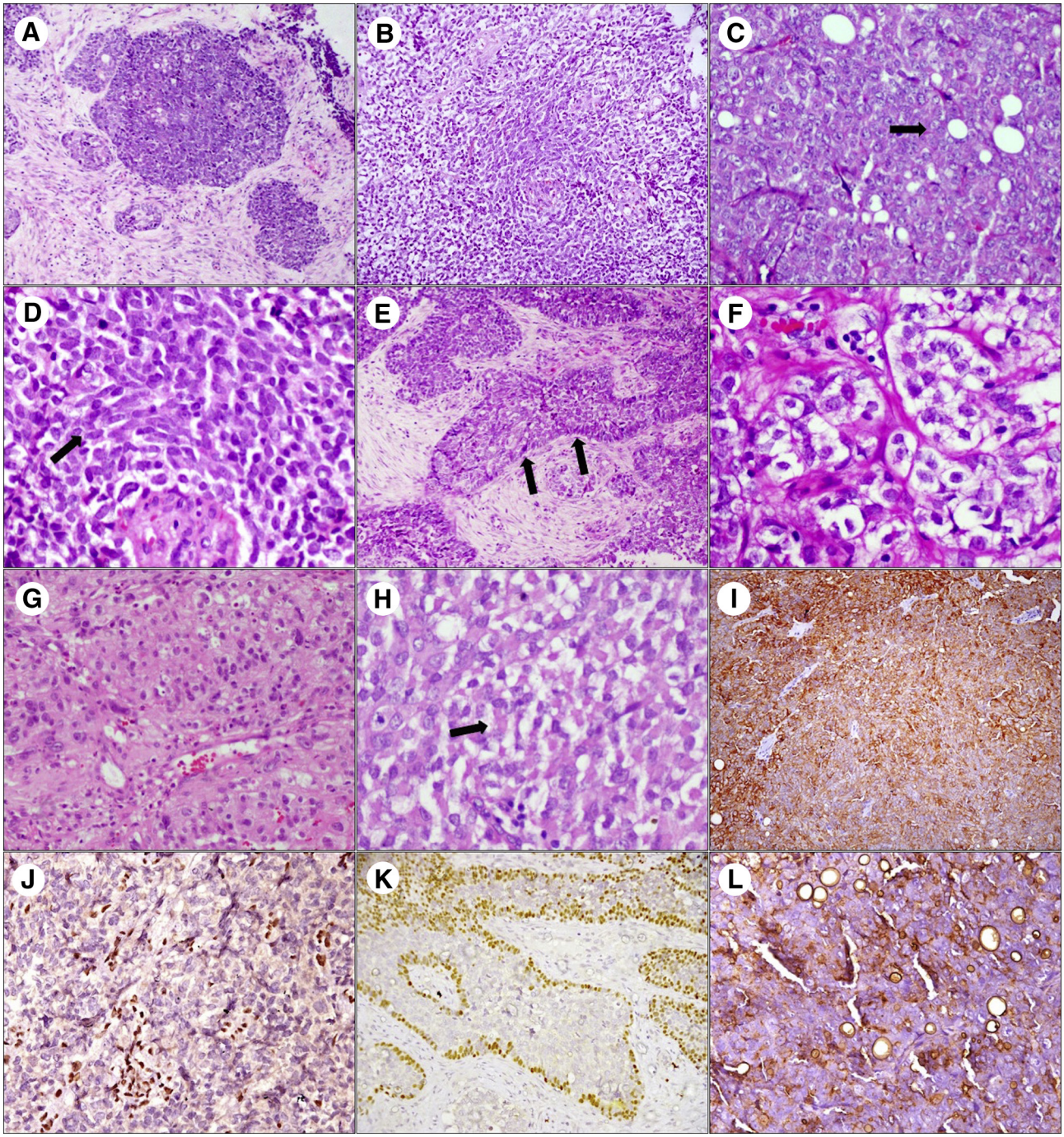

Fig. 2 Morphologic features of SDSC. Basaloid-appearing tumor with cells in nests (A; hematoxylin and eosin [HE], original magnification ×100) and sheets (B; HE, ×200). Tumor cells showing cytoplasmic empty vacuoles (arrow; C; HE, ×200), spindled nuclei (arrow; D; HE, ×400), peripheral palisading of nuclei (arrows; E; HE, ×200), and clear cytoplasm (F; HE, ×400). Plasmacytoid/rhabdoid predominant tumor composed of sheets of cells with abundant eosinophilic cytoplasm (G; HE, ×200) and rhabdoid cells (arrow; H; HE, ×400). Tumor cells are immunopositive for pancytokeratin (I; IHC, ×100) and show loss of INI1 (J; IHC, ×200). p40 positivity in case 2 (K; IHC, ×200). Epithelial membrane antigen highlights empty vacuoles (L; IHC ×200).

2. Materials and methods

This study performed on archival patient tumor samples received approval from the Institute Ethics Committee. All cases reported as sinonasal carcinomas, including sinonasal undifferentiated carcinoma (SNUC), poorly differentiated carcinoma, undifferentiated carcinoma, poorly differentiated SCC, and adenocarcinoma, between 2009 and 2017 were retrieved from our

surgical pathology archives. Histopathologic and immunohistochemical features were reviewed. IHC for SMARCB1 (INI1) was performed on formalin-fixed, paraffin-embedded tumor sections, using a mouse monoclonal primary antibody (clone MRQ-27; Cell Marque, Rocklin, CA) in a dilution of 1:50. Sections from normal tonsil were used as positive controls; endothelial cell nuclei served as internal positive controls. Cases with loss of nuclear staining for INI1 were interpreted as INI1 deficient. IHC for cyclin D1 (1:100; Biocare Medical, Concord, CA) was performed in all INI1-deficient cases, and a labeling index was calculated, as described previously [13]. Clinical details and follow-up of these cases were obtained, where available, by retrospective chart review and telephonic interview.

3. Results

Two hundred twenty-five such cases of sinonasal carcinomas were identified from our archives and were evaluated for INI1 expression. Thirteen cases (5.8%) showed loss of nuclear expression of INI1. Clinical details, treatment, and follow-up of patients are summarized in Table 1. Biopsy and resection specimens were available for patients 1 and 5, whereas the remaining patients had a single tissue sample. Patients ranged in age from 11 to 65 years (mean, 42 years; median, 40 years) and included 11 males and 2 females (male-to-female ratio, 5.5:1). Three cases (23.1%) had originally been diagnosed as SNUC, 3 cases (23.1%) as adenocarcinoma, 2 (15.4%) as poorly differentiated carcinoma, and 2 (15.4%) as poorly differentiated SCC. Based on histopathologic features of the initial biopsy from patient 5, the diagnosis of SDSC was considered upfront and was confirmed on INI1 staining. Patient 12 had undergone excision of a maxillary mass elsewhere 1 year before presentation at our Institute; details of the procedure and histopathology diagnosis were not available for the same. We received a biopsy from the recurrent tumor in the maxillary antrum and medial wall, which was diagnosed upfront as SDSC (Fig. 1). Patient 13 underwent a biopsy in Nepal, which was reported as olfactory

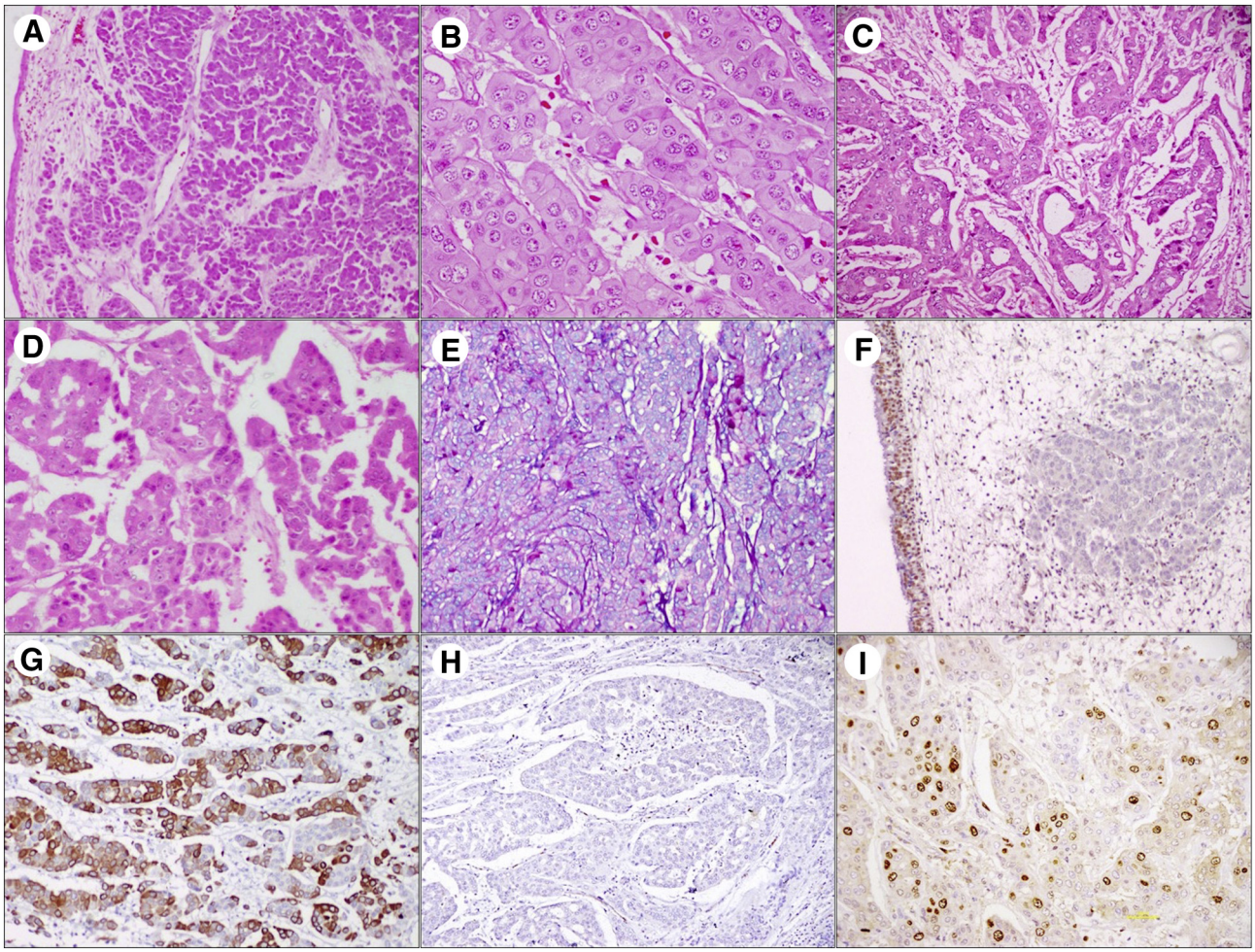

Fig. 3 Oncocytoid adenocarcinoma–like pattern. Pink-appearing tumor (A; hematoxylin and eosin [HE], original magnification ×100) composed of cuboidal cells with abundant eosinophilic cytoplasm and central round vesicular nuclei (B; HE, ×400), gland-like structures (C; HE, ×200), and prominent nucleoli (D; HE, ×400). Tumor cells lack mucin (E; Alcian blue–PAS, ×200), show loss of INI-1 (F; IHC, ×200), are positive for CK7 (G; IHC, ×200) and negative for CK20 (h; IHC, ×100), and show high Ki-67 labeling (I; IHC, ×200).

Table 2 Histopathologic features of cases of *SMARCB1*-deficient sinonasal carcinoma

Case no.	Predominant pattern	Architecture	Overlying mucosa	Empty vacuoles	Peripheral palisading	Clear cytoplasm	Ovoid nuclei	Nucleoli	Intracytoplasmic mucin	Inflammatory cells
1	Basaloid	Sheets	N/A	Present	Absent	Present	Present	Present	Absent	Lymphocytes
2	Basaloid	Inverted papilloma–like	N/A	Occasional	Present	Present	Absent	Absent	Absent	Absent
3	Oncocytoid adenocarcinoma–like	Nests, cords, glands	Normal	Absent	Absent	Absent	Absent	Present	Absent	Foamy histiocytes
4	Plasmacytoid/rhabdoid	Sheets, nests	Normal	Absent	Absent	Present	Absent	Absent	Absent	Absent
5	Basaloid	Sheets, islands	Normal	Numerous	Present	Present	Absent	Present	Absent	Foamy histiocytes
6	Plasmacytoid/rhabdoid	Sheets, islands	N/A	Absent	Absent	Present	Absent	Absent	Absent	Absent
7	Plasmacytoid/rhabdoid	Nests, islands	Normal	Absent	Present	Absent	Absent	Absent	Absent	Lymphocytes
8	Basaloid	Sheets	N/A	Absent	Absent	Present	Present	Absent	Absent	Absent
9	Plasmacytoid/rhabdoid	Islands	N/A	Absent	Absent	Present	Absent	Present	Absent	Absent
10	Basaloid	Sheets, nests, cords	N/A	Occasional	Absent	Absent	Absent	Present	Absent	Lymphocytes, neutrophils
11	Oncocytoid adenocarcinoma–like	Glands, nests, trabeculae	Normal	Absent	Absent	Absent	Absent	Present	Absent	Absent
12	Basaloid	Sheets	N/A	Present	Absent	Absent	Present	Present	Absent	Neutrophils
13	Plasmacytoid/rhabdoid	Sheets, lobules	Normal	Occasional	Absent	Absent	Absent	Present	Absent	Lymphocytes, plasma cells

Abbreviation: N/A, not available.

neuroblastoma with rhabdomyoblastic differentiation, after which he was referred to our Institute; the biopsy block was submitted for review and was diagnosed as SDSC.

On histologic examination, most cases (6/13; 46.2%) showed basaloid morphology (Fig. 2A-F), with predominantly undifferentiated cells having scant cytoplasm arranged in sheets, nests, and islands with minimal intervening desmoplastic stroma. Inverted papilloma–like downward growth was seen in 1 case (7.7%). Variable proportion of cells with rhabdoid morphology, having abundant eosinophilic cytoplasm and eccentric nuclei, was seen interspersed between the basaloid cells in all these cases. Tumor cells with a predominant plasmacytoid/rhabdoid population of cells (Fig. 2G and H) accounted for 38.5% of cases (5/13). Clear, empty-appearing cytoplasmic vacuoles were seen in 6 cases (46.2%), 5 with basaloid and 1 with plasmacytoid/rhabdoid appearance. Palisading of cells at the periphery of nests and islands was seen in 3 cases (23.1%). Three basaloid-appearing tumors showed focal presence of spindle-shaped cells with ovoid to elongated nuclei; frank sarcomatoid features were, however, absent.

Two cases (Fig. 3) comprised large cuboidal to polygonal cells with well-demarcated cytoplasmic borders, abundant eosinophilic cytoplasm, and large round vesicular nuclei having variably prominent nucleoli. These oncocytoid, almost hepatoid-appearing, cells were arranged in nests, cords, and trabeculae and also displayed gland-like structures with well-defined lumina. Cells lining these glands showed cilia at the luminal aspect at places. Alcian blue–periodic acid–Schiff (PAS) did not reveal the presence of mucin, either luminal or intracytoplasmic. Histopathologic features of all the cases are summarized in Table 2.

Immunohistochemically, all cases were immunopositive for pancytokeratin. None of the cases showed p16, NUT, or mic2 positivity. p40 staining, when present (2 cases), was focal, staining nuclei at the periphery of tumor islands. Epithelial membrane antigen highlighted the cytoplasmic empty vacuoles. Strong CD34 positivity was seen in case 12 in approximately 75% of tumor cells (Figs. 3H and 4). Among neuroendocrine markers, focal synaptophysin and chromogranin positivity was seen in 1 case each; CD56 was negative. Among the oncocytoid adenocarcinoma–like cases, one showed CK7 positivity, whereas the other was negative; CK20 was negative, as were organ-specific markers for adenocarcinomas viz TTF-1, CDX2, and prostate specific antigen. On cyclin D1 IHC (Fig. 4), faint nuclear immunopositivity for cyclin D1 was seen only focally in 3 cases, with labeling index in areas showing highest positivity ranging from 1% to 10%. None of the cases showed strong diffuse cyclin D1 immunostaining.

Follow-up was available for 5 (38%) out of 13 patients, which is a limiting factor of our study. Ours being the apex

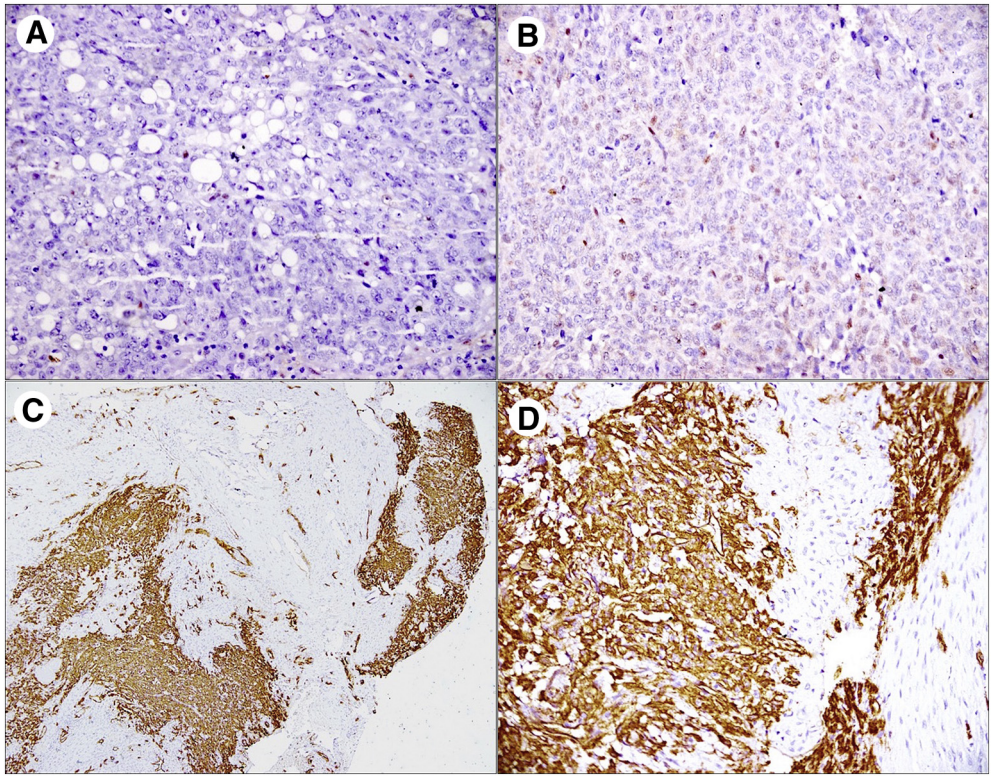

Fig. 4 Cyclin D1 and CD34 immunoexpression. Case 1 showing tumor cells devoid of cyclin D1 staining (A; IHC, original magnification ×200). Case 5 showing focal faint cyclin D1 positivity (B; IHC, ×200). Case 12 showing diffuse CD34 immunopositivity (C; IHC, ×40; D; IHC ×200).

tertiary care center in the country where health care is provided at markedly subsidized cost, patient load is high and there is a considerable waiting period for surgery and radiotherapy. Thus, the patient attrition rate is significant, as once a tissue diagnosis has been established, patients revert to regional cancer centers to receive treatment. Of the 5, 2 patients (1 and 4) received platinum-based neoadjuvant chemotherapy (NACT), which led to reduction in tumor size in both. Patient 1 then underwent radical maxillectomy and received postoperative radiotherapy (PORT), leading to clinical remission. He was disease-free at last follow-up. Patient 4 was referred to his local hospital for surgery and PORT. Patient 5 underwent complete resection of the tumor and received platinum-based chemotherapy followed by PORT, after which there was no evidence of disease at 8 months. Patient 12 was to receive palliative chemotherapy (CT) after biopsy, but he died of excessive bleeding from the mass. Patient 13 has been diagnosed recently and is scheduled for NACT followed by craniofacial resection and postoperative chemoradiation.

4. Discussion

Loss of expression of *SMARCB1*, a member of SWI/SNF family of chromatin remodeling genes, is seen in several malignancies, including RTs of the central nervous system, that is, AT/RTs, kidneys, and soft tissues, as well as in other tumors such as epithelioid sarcoma, renal medullary carcinomas, epithelioid malignant peripheral nerve sheath tumor, extraskeletal myxoid chondrosarcoma, myoepithelial carcinoma, and atypical chordoma [9,14]. INI1 IHC serves as a valuable tool for identification of these tumors. Loss of *SMARCB1* in sinonasal tumors was first described almost simultaneously by 2 groups: Agaimy et al [5] described a series of 3 cases of *SMARCB1* (INI1)–deficient basaloid sinonasal carcinoma, as did Bishop et al [6] in their report of 9 such cases. These tumors occurred over a wide age range, showed a distinct growth pattern with focal presence of rhabdoid cells, and showed absence of INI1 staining. Subsequently, around 60 cases of this unique neoplasm have been reported in the English literature, all from Western countries, barring one from China [7,9,14-17]. They have been found to account for 2.7% to 7% of all primary sinonasal carcinomas assessed [5,6,14]. These patients ranged in age from 16 to 89 years with mean age in the sixth decade and included an almost equal proportion of males and females [6,7,9,14,15,18]. Most had previously been diagnosed as having nonkeratinizing SCC or SNUC [6,7]. Our results are similar to these; however, one of our patients was an 11-year-old child, the youngest patient to be reported. The sex distribution of our patients is, however, strikingly different, with a definite male preponderance.

Although initial reports characterized SDSCs as poorly differentiated basaloid-appearing neoplasms lacking evident squamous

or glandular differentiation, since then the spectrum of morphologic features of SDSC has gradually broadened [7]. Most SDSCs fall into the broad morphologic categories of basaloid "blue cell" tumors or plasmacytoid/rhabdoid "pink cell" tumors. Basaloid tumors are characterized by undifferentiated tumor cells with high nuclear/cytoplasmic ratio, scant cytoplasm, and minimal nuclear pleomorphism arranged in sheets or nests in a desmoplastic stroma [6]. A variable proportion of plasmacytoid/rhabdoid-appearing cells with eccentric nuclei and eosinophilic inclusion-like cytoplasm, the morphologic hallmark of INI1 deficient neoplasms, may be seen dispersed singly in basaloid tumors. Pink cell tumors, on the other hand, consist predominantly of such plasmacytoid/rhabdoid cells arranged in sheets [7]. Other features that have been described include inverted papilloma–like downward growth, peripheral palisading, pagetoid spread into the overlying respiratory mucosa, presence of clear cells, and presence of nonspecific empty vacuoles [5-7,17]. Although most of our cases were diagnosed retrospectively, 2 cases were diagnosed prospectively based on the identification of occasional rhabdoid cells and empty vacuoles in a basaloid appearing neoplasm, and 1 case was composed predominantly of plasmacytoid/rhabdoid cells, prompting INI1 IHC, which showed loss of expression.

Two of our cases were composed entirely of "oncocytoid" cells with abundant glassy cytoplasm, having centrally placed, round vesicular nuclei with prominent eosinophilic nucleoli. Interestingly, both these cases showed the presence of well-formed tubular/glandular structures, apart from nests and cords of tumor cells. This oncocytoid adenocarcinoma–like (mucin being absent) appearance has not been described previously. Because of their tubuloglandular morphology, these cases had originally each been diagnosed as nonintestinal type adenocarcinoma and poorly differentiated adenocarcinoma. Agaimy et al [7] identified "oncocytic squamoid cells" with acantholytic appearance in 3 cases; however, these cases did not show the presence of gland-forming structures. Glandular architecture leading to diagnosis of adenocarcinoma has rarely been described previously in 5 cases [7,9]. Two of these had predominant plasmacytoid/rhabdoid appearance, whereas 1 had basaloid predominant appearance [7]; for the remaining 2, these details were not available.

Although SDSCs are consistently immunopositive with pancytokeratin, focal and variable positivity for HMWCK, p63, p40, and neuroendocrine markers has been described [6,7,15]. Unlike central nervous system and soft tissue RTs, SDSCs do not show a polyphenotypic immunoexpression profile, highlighting their distinctness from these clinical entities. Genetic analysis of SDSCs has shown that around three-fourths harbor either homozygous or heterozygous deletions of the *SMARCB1* locus as detected by fluorescent in situ hybridization [6,7]. Associated monosomy 22q has also been identified [7]. It has been suggested that monoallelic or biallelic intragenic gene mutations, small deletions below the resolution of fluorescent in situ hybridization, or epigenetic mechanisms are responsible for loss of INI1 expression in the remaining cases, which do not show *SMARCB1* deletion [7].

Differential diagnosis includes poorly differentiated and undifferentiated carcinomas such as nonkeratinized SCC, small cell neuroendocrine carcinoma, NUT carcinoma, adamantinoma-like Ewing sarcoma, SNUC, and adenocarcinoma. Nonkeratinized SCCs exhibit greater nuclear pleomorphism than SDSC, and surface dysplasia is frequently present [17]. The former show diffuse, strong p63 and p40 staining, which is variable in the latter [15]. Small cell neuroendocrine carcinomas have scant cytoplasm and nuclei lacking nucleoli and display nuclear molding; they stain positively with at least 2 neuroendocrine markers, including synaptophysin, chromogranin, and CD56, along with dot-like cytokeratin positivity [19]. Although SDSC may show neuroendocrine marker positivity, staining is usually focal and not seen with all the markers [17]. NUT carcinomas are composed of undifferentiated basaloid cells; abrupt keratinization, though characteristic, may not always be present, especially in small biopsies [4]. Strong p40 staining and nuclear NUT staining help to distinguish it from SDSC. Adamantinoma-like Ewing sarcoma comprises p40/p63-positive basaloid cells, which show peripheral palisading, leading to an overlap with SDSC. Membranous CD99 and nuclear FLI1 positivity, characteristic of the former, is not seen in SDSC [19]. SNUC is a diagnosis of exclusion and shows undifferentiated histomorphology and IHC profile similar to basaloid "blue" SDSC, and can be differentiated from the latter by INI1 staining only. SDSC with glandular architecture should be differentiated from sinonasal adenocarcinoma, both intestinal-type (ITAC) and non–intestinal-type (non-ITAC). ITAC is composed of mucinous cells and goblet cells similar to colonic adenocarcinoma; strong CK20, CDX2, and villin positivities, along with variable CK7 staining and retained INI1, help differentiate from SDSC [20]. Non-ITACs contain intracytoplasmic or intraluminal mucin that is highlighted by PAS [21]. Although non-ITACs share CK7 positivity with SDSC with adenocarcinoma morphology, as seen in one of our cases, INI1 is retained. Thus, INI1 is an extremely valuable adjunct in the differential diagnosis of poorly differentiated sinonasal carcinomas and should routinely be incorporated into IHC panels for their evaluation.

Similar to *SMARB1*/INI1-deficient tumors at other locations, SDSCs are aggressive tumors with uniformly poor prognosis, as most present with large, locally advanced, destructive masses [6,9,15]. Although no defined management protocols are available, most patients have been treated with surgery followed by adjuvant chemoradiation [6,7,15]. Local recurrences and distant metastases are frequent after treatment, with 37% patients in the largest series developing distant metastases and 33% of patients developing locoregional recurrence [5-7,15].

Wasserman et al [17] reported good response to cisplatin-based NACT with significant reduction in tumor bulk, as also seen in 2 of our cases. However, although NACT seems to help in preoperative reduction in tumor size facilitating complete excision and in improving locoregional control, distant metastases to the lung, pleura, bone, and liver have been reported after NACT and radical surgery [17].

Lack of effective treatment regimens for SDSC demands the identification of novel targeted therapeutic agents. The product of the INI1 gene interacts with several key cell signaling molecules, thus regulating the transcription of downstream target genes and modulating cellular response to growth and differentiation factors. Cyclin D1 is one such critical downstream target gene to whose promoter INI1 binds and thus regulates its expression [22]. Loss of INI1 expression leads to up-regulation of cyclin D1, resulting in cell-cycle progression, which is a requisite for neoplastic proliferation [11]. This derepression of cyclin D1 expression consequent to loss of SMARCB1 has led to exploration of cyclin D1 inhibitors for management of RTs, and positive results have been obtained in animal models [22,23]. We have previously demonstrated cyclin D1 overexpression in AT/RTs showing INI1 loss [13]. We therefore performed cyclin D1 immunostaining in our SDSC cases to identify cyclin D1 overexpression as a marker for tumors that might respond to treatment with cyclin D1 inhibitors. However, none of our cases showed strong immunoexpression of cyclin D1. Because cyclin D1 is a component of many cellular pathways, it is likely that other genetic or epigenetic alterations may be preventing overexpression of cyclin D1 despite loss of SMARCB1, and further studies need to be undertaken to evaluate the same. Indeed, epigenetic alterations in the form of promoter methylation of RASSF1α gene have already been reported in SDSCs [14]. Occasional researchers have suggested that SDSCs be classified as RTs, based on SMARCB1 loss. The absence of cyclin D1 overexpression in SDSC as opposed to that in RTs highlights the differences in pathogenetic mechanisms of these 2 neoplasms and serves to establish it further as a unique entity.

5. Conclusions

SDSC is a rare, emerging entity that has the morphologic appearance of a poorly differentiated carcinoma. Presence of cells with basaloid, rhabdoid, and oncocytoid morphology, with or without clear vacuoles, in an undifferentiated sinonasal tumor should prompt the use of INI1 IHC for its identification and differentiation from other poorly differentiated carcinomas, particularly SNUC, which is imperative bearing in mind the aggressive clinical course of the former.

References

[1] Bishop JA, Westra WH. NUT midline carcinomas of the sinonasal tract. Am J Surg Pathol 2012;36:1216-21.

[2] Bishop JA, Ogawa T, Stelow EB, et al. Human papillomavirus–related carcinoma with adenoid cystic-like features: a peculiar variant of head and neck cancer restricted to the sinonasal tract. Am J Surg Pathol 2013;37:836-44.

[3] Bishop JA. Recently described neoplasms of the sinonasal tract. Semin Diagn Pathol 2016;33:62-70.

[4] Kakkar A, Antony VM, Irugu DVK, Adhikari N, Jain D. NUT midline carcinoma: a series of five cases, including one with unusual clinical course. Head Neck Pathol 2018;12:230-6.

[5] Agaimy A, Koch M, Lell M, et al. SMARCB1(INI1)-deficient sinonasal basaloid carcinoma: a novel member of the expanding family of SMARCB1-deficient neoplasms. Am J Surg Pathol 2014;38:1274-81.

[6] Bishop JA, Antonescu CR, Westra WH. SMARCB1 (INI-1)-deficient carcinomas of the sinonasal tract. Am J Surg Pathol 2014;38:1282-9.

[7] Agaimy A, Hartmann A, Antonescu CR, et al. SMARCB1 (INI-1)-deficient sinonasal carcinoma: a series of 39 cases expanding the morphologic and clinicopathologic spectrum of a recently described entity. Am J Surg Pathol 2017;41:458-71.

[8] Zeng M, Chen C, Yang S, Chen X. SMARCB1 (INI1)–deficient sinonasal carcinoma: a newly described entity. Int J Clin Exp Pathol 2016;9:3454-8.

[9] Shatzkes DR, Ginsberg LE, Wong M, et al. Imaging appearance of SMARCB1 (INI1)–deficient sinonasal carcinoma: a newly described sinonasal malignancy. AJNR Am J Neuroradiol 2016;37:1925-9.

[10] Versteege I, Medjkane S, Rouillard D, Delattre O. A key role of the hSNF5/INI1 tumor suppressor in the control of the G1-S transition of the cell cycle. Oncogene 2002;21:6403-12.

[11] Zhang ZK, Davies KP, Allen J, et al. Cell cycle arrest and repression of cyclin D1 transcription by INI1/hSNF5. Mol Cell Biol 2002;22:5975-88.

[12] Smith ME, Cimica V, Chinni S, et al. Therapeutically targeting cyclin D1 in primary tumors arising from loss of Ini1. Proc Natl Acad Sci U S A 2011;108:319-24.

[13] Kakkar A, Biswas A, Goyal N, et al. The expression of cyclin D1, VEGF, EZH2, and H3K27me3 in atypical teratoid/rhabdoid tumors of the CNS: a possible role in targeted therapy. Appl Immunohistochem Mol Morphol 2016;24:729-37.

[14] Laco J, Chmelařová M, Vošmiková H, et al. SMARCB1/INI1-deficient sinonasal carcinoma shows methylation of RASSF1 gene: a clinicopathological, immunohistochemical and molecular genetic study of a recently described entity. Pathol Res Pract 2017;213:133-42.

[15] Bell D, Hanna EY, Agaimy A, Weissferdt A. Reappraisal of sinonasal undifferentiated carcinoma: SMARCB1 (INI1)–deficient sinonasal carcinoma: a single-institution experience. Virchows Arch 2015;467:649-56.

[16] Allison DB, Bishop JA, Ali SZ. Cytopathologic characteristics of SMARCB1 (INI-1) deficient sinonasal carcinoma: a potential diagnostic pitfall. Diagn Cytopathol 2016;44:700-3.

[17] Wasserman JK, Dickson BC, Perez-Ordonez B, de Almeida JR, Irish JC, Weinreb I. INI1 (SMARCB1)-deficient sinonasal carcinoma: a clinicopathologic report of 2 cases. Head Neck Pathol 2017;11:256-61.

[18] Barresi V, Branca G, Raso A, Mascelli S, Caffo M, Tuccari G. Atypical teratoid rhabdoid tumor involving the nasal cavities and anterior skull base. Neuropathology 2016;36:283-9.

[19] Rooper LM, Westra WH. A protein lost, a diagnosis gained: a review of SMARCB1-deficient sinonasal carcinomas. AJSP Rev Rep 2018;23:13-8.

[20] Stelow EB, Franchi A, Wenig BM. Intestinal-type adenocarcinoma. In: El-Naggar AK, Chan JKC, Grandis JR, Takata T, Slootweg PJ, editors. WHO Classification of Head and Neck Tumours. Lyon: IARC; 2017. p. 23-4.

[21] Stelow EB, Brandwein-Gensler M, Franchi A, Nicolai P, Wenig BM. Non–intestinal-type adenocarcinoma. In: El-Naggar AK, Chan JKC, Grandis JR, Takata T, Slootweg PJ, editors. WHO Classification of Head and Neck Tumours. Lyon: IARC; 2017. p. 24-6.

[22] Alarcon-Vargas D, Zhang Z, Agarwal B, Challagulla K, Mani S, Kalpana GV. Targeting cyclin D1, a downstream effector of INI1/hSNF5, in rhabdoid tumors. Oncogene 2006;25:722-34.

[23] Smith ME, Das BC, Kalpana GV. In vitro activities of novel 4-HPR derivatives on a panel of rhabdoid and other tumor cell lines. Cancer Cell Int 2011;11:34.